Available online at www.sciencedirect.com
SCIENCE DIRECT
International Journal of Heat and Mass Transfer 49 (2006) 207–218
International Journal of HEAT and MASS TRANSFER
www.elsevier.com/locate/ijhmt

Experimental study of evaporation heat transfer characteristics of refrigerants R-134a and R-407C in horizontal small tubes

Y.M. Lie, F.Q. Su, R.L. Lai, T.F. Lin *

Department of Mechanical Engineering, National Chiao Tung University, Hsinchu 30010, Taiwan, ROC

Received 2 December 2004; received in revised form 30 July 2005
Available online 27 September 2005

Abstract

An experiment is carried out here to investigate the characteristics of the evaporation heat transfer for refrigerants R-134a and R-407C flowing in horizontal small tubes having the same inside diameter of 0.83 or 2.0 mm. In the experiment for the 2.0-mm tubes, the refrigerant mass flux G is varied from 200 to 400 kg/m^2 s, imposed heat flux q from 5 to 15 kW/m^2, inlet vapor quality x_{in} from 0.2 to 0.8 and refrigerant saturation temperature T_{sat} from 5 to 15 °C. While for the 0.83-mm tubes, G is varied from 800 to 1500 kg/m^2 s with the other parameters varied in the same ranges as those for $D_i = 2.0$ mm. In the study the effects of the refrigerant vapor quality, mass flux, saturation temperature and imposed heat flux on the measured evaporation heat transfer coefficient h_r are examined in detail. The experimental data clearly show that both the R-134a and R-407C evaporation heat transfer coefficients increase almost linearly and significantly with the vapor quality of the refrigerant, except at low mass flux and high heat flux. Besides, the evaporation heat transfer coefficients also increase substantially with the rises in the imposed heat flux, refrigerant mass flux and saturation temperature. At low R-134a mass flux and high imposed heat flux the evaporation heat transfer coefficient in the smaller tubes ($D_i = 0.83$ mm) may decline at increasing vapor quality when the quality is high, due to the partial dryout of the refrigerant flow in the smaller tubes at these conditions. We also note that under the same x_{in}, T_{sat}, G, q and D_i, refrigerant R-407C has a higher h_r when compared with that for R-134a. Finally, an empirical correlation for the R-134a and R-407C evaporation heat transfer coefficients in the small tubes is proposed.
© 2005 Elsevier Ltd. All rights reserved.

1. Introduction

In the past decade following the signing of the Montreal Protocol in 1996, extensive research has been undertaken to search for the alternatives that can replace the chlorofluorocarbons (CFCs) refrigerants. It was well known at that time that the use of the CFCs refrigerants, which contain chlorine and carbon, would lead to the ozone depletion and a consequent increase in ultraviolet radiation, and would cause global warming. Some hydrochlorofluorocarbons (HCFCs) and hydrofluorocarbons (HFCs) refrigerants have been developed. The HCFCs refrigerants contain less chlorine than the CFCs and have shorter atmospheric life time. They were considered as interim for the CFCs. The HFCs refrigerants have zero ozone depletion potential

* Corresponding author. Tel.: +886 35 712121 55118; fax: +886 35 726 440.
E-mail address: tflin@mail.nctu.edu.tw (T.F. Lin).

0017-9310/$ - see front matter © 2005 Elsevier Ltd. All rights reserved.
doi:10.1016/j.ijheatmasstransfer.2005.07.018

Nomenclature

A_s	inside surface area of the small tubes, m^2
Bo	Boiling number, $Bo = \frac{q}{G \cdot i_{fg}}$, dimensionless
D_h	hydraulic diameter, mm
D_i	diameter of small tube, mm
f	friction factor, dimensionless
g	gravitational acceleration, m/s^2
G	mass flux, kg/m^2 s
h_l	single-phase liquid heat transfer coefficient, W/m^2 °C
h_r	evaporation heat transfer coefficient, W/m^2 °C
i_{fg}	enthalpy of vaporization, J/kg
k	thermal conductivity, W/mK
N_{conf}	confinement number, $N_{conf} = \frac{\left[\frac{\sigma}{g(\rho_l-\rho_g)}\right]^{0.5}}{D_h}$, dimensionless
Nu_l	Nusselt number for liquid flow, $Nu_l = \frac{h_l D_i}{k_l}$, dimensionless
Nu_r	Nusselt number for evaporation, $Nu_r = \frac{h_r D_i}{k_l}$, dimensionless
Pr	Prandtl number, dimensionless
q	average imposed heat flux, W/m^2
Q	heat transfer rate, W
Re	Reynolds number, $Re = \frac{G \cdot D_i}{\mu_l}$, dimensionless
T	temperature, °C
$T_{r,sat}$	saturated temperature of refrigerant, °C
x	vapor quality

Greek symbols

Δx	total quality change in the small tubes
μ	viscosity, N s/m^2
ρ	density, kg/m^3
σ	surface tension, N/m

Subscripts

g	vapor phase
in	at inlet of the test section
l	liquid phase
n	net power input to the refrigerant R-134a or R-407C
r	refrigerant
sat	saturation
wall	the inner wall of small tubes

and can replace the CFCs for some period of time. In order to properly use these new refrigerants, we need to understand their thermodynamic, flow and heat transfer properties. In particular, a detailed understanding of the characteristics of the evaporation and condensation heat transfer for the HFCs refrigerants is very important in the design of evaporators and condensers for many refrigeration and air conditioning systems.

Recently, there is growing interest in the use of ultra-compact heat exchangers in various thermal systems because of their very high heat transfer density. Thus the flow and heat transfer characteristics in small and capillary tubes have been extensively investigated for various fluids such as air, water and some refrigerants [1]. But the heat transfer characteristics associated with the evaporation and condensation of the HFCs refrigerants in the small tubes are less explored. Data for these two-phase heat transfer coefficients in the small tubes are still scarce. In the present study we conduct experiments to measure the evaporation heat transfer coefficients of the HFCs refrigerants R-134a and R-407C in small tubes. We choose these two refrigerants in this study because they are regarded as the major substitutes for refrigerants R-12 and R-22.

In what follows the relevant literature on the present study is briefly reviewed. Yu et al. [2] recently examined flow boiling heat transfer for water in a 2.98-mm diameter channel and found that the measured boiling heat transfer coefficients for the vapor quality above 0.5 depended on the heat flux but were independent of the water mass flux. They concluded that the nucleate boiling was dominant over the convective boiling in small channels. The results are significantly different from these for the conventional channels, where the mass flux effects can be substantial. Similarly, Sumith et al. [3] measured the saturated flow boiling heat transfer and pressure drop of water in a test section made of a stainless steel tube with an inner diameter of 1.45 mm. They indicated that the dominant flow pattern in the tube was a slug-annular or an annular flow, and liquid film evaporation dominated the heat transfer.

An experiment carried out by Yan and Lin [4,5] to study the evaporation heat transfer and pressure drop of R-134a in a tube bank forming by 28 small side-by-side contacting pipes ($D_i = 2.0$ mm) revealed that both the refrigerant mass flux and imposed heat flux were important and the evaporation heat transfer in the small pipes was significantly higher than that in large tubes. A similar study for subcooled flow boiling of R-134a in a vertical multiport parallel rectangular channels ($D_h = 2.01$ mm) was carried out by Agostini and Bontemps [6]. In a visualization investigation Nino et al. [7] examined R-134a flow boiling in a multiport mini-channel tube with $D_h = 1.5$ mm. They proposed a method to describe the fraction of time or the probability that a flow pattern existed in a particular flow condition. A recent study from Fujita et al. [8] for R-123 boiling in a horizontal small tube with an inside diameter of

1.12 mm suggested that heat transfer in the flow was dominated by the nucleate boiling and the effects of the refrigerant mass flux and vapor quality to the boiling heat transfer were very weak. A similar study for R-113 boiling conducted by Lazarek and Black [9] noted the negligible variation of the boiling heat transfer coefficient with the local vapor quality, which implied that the wall heat transfer processes were again controlled by nucleate boiling. In a vertical small tube ($D_i = 1$ mm) with refrigerant R-141b flowing in it, Lin et al. [10] found that at low quality, nucleate boiling dominated. But at higher quality, convection dominated. In a further study [11], they examined the same refrigerant in four circular tubes with diameters 1.1, 1.8, 2.8, 3.6 mm and one square tube of cross-section 2×2 mm^2. Their results indicate that the mean heat transfer coefficient in a tube or channel is independent of the mass flux and tube diameter but is a function of the imposed heat flux. Cornwell and Kew [12] observed boiling in refrigerant R-113 flow and measured the heat transfer for two geometries: one had 75 channels with $D_h = 1.03$ mm and other had 36 channels with $D_h = 1.64$ mm. Their experimental work suggested the presence of three two-phase flow patterns in the channels: isolated bubble, confined bubble and annular-slug flow. In a continuing study [13], they investigated refrigerant R-141b boiling in a horizontal tube with its inner diameter ranging from 1.39 to 3.69 mm and proposed that flow boiling in a narrow channel might be through one of four mechanisms: nucleate boiling, confined bubble boiling, convective boiling and partial dry-out. They further indicated that, except at very low heat flux, the boiling showed a strong dependence on the heat flux, a weak dependence on the mass flux, and independence of the quality. Besides, they introduced a new dimensionless group named as the confinement number N_{conf}, which represented the importance of the restriction of the flow by the small size of the channel. The dimensionless number N_{conf} can be used to find the transition from the isolated to confined bubble regimes. To a first approximation, they showed that the confined boiling occurred when $N_{conf} > 0.5$.

By examining boiling of refrigerants in a small circular tube ($D_i = 2.46$ mm) and a rectangular duct ($D_h = 2.40$ mm) with nearly the same hydraulic diameters, Tran et al. [14] showed that there was no significant geometry effect for the two channels tested. Furthermore, their results imply that the nucleation mechanism dominates over the convection mechanism in small-channel evaporators over the full range of quality (0.2–0.8), which is contrary to the situations in larger channels where the convection mechanism dominates at qualities typically above 0.2. Bao et al. [15] also found that the boiling heat transfer coefficient was a strong function of the heat flux and system pressure in a 1.95 mm diameter tube with R-11 and R-123, while the effects of the mass flux and vapor quality were very small, suggesting that the heat transfer was mainly through the nucleate boiling. Wambsganss et al. [16] studied boiling heat transfer of refrigerant R-113 in a small diameter (2.92 mm) tube and evaluated 10 different heat transfer correlations. They found that the high boiling number and slug flow pattern led to the domination by the nucleation mechanism and the two-phase correlations based on this dominance also predicted the data best. Moreover, Warrier et al. [17] tested FC-84 in five parallel channels with each channel having a hydraulic diameter of 0.75 mm and compared their results with five widely used correlations. They then proposed two new correlations, one for subcooled flow boiling heat transfer and another for saturated flow boiling heat transfer. Oh et al. [18] examined R-134a in capillary tubes of 500-mm long and 2, 1 and 0.75-mm inside diameters. They concluded that the heat transfer in the forced convective boiling was more influenced by the refrigerant mass flux than by the boiling number and the heat transfer coefficient was controlled by the Reynolds number of the flow. Besides, their results also showed that the dry-out point moved to the lower quality with decreasing size of the tubes. Vaporization of CO_2 in 25 flowchannels each having an inside diameter of 0.8 mm was recently examined by Pettersen [19]. He also observed the two-phase flow pattern with another separate test rig with a 0.98-mm heated glass tube. The results showed that nucleate boiling dominated at low/moderate vapor fractions, where the boiling heat transfer coefficient increased with the heat flux and refrigerant saturated temperature but was less affected by the mass flux and vapor fraction. Moreover, the dryout effects became very important at higher mass flux and temperature, where the boiling heat transfer coefficient dropped rapidly at increasing quality. And the two-phase flow was in intermittent and annular flow regimes, the latter becoming more important at high mass flux. More complete information on various aspects of the two phase flow and boiling heat transfer in ultra-compact evaporators and microchannels is available from the recent critical review conducted by Kim et al. [1], Ghiaasiaan and Abdel-khalik [20], Thome [21], Sobhan and Garimella [22], Kandlikar [23,24], Watel [25], and Vlasie et al. [26].

The above literature review clearly indicates that the experimental data for the evaporation heat transfer of the HFC refrigerants in small tubes are still in urgent need. To complement our earlier investigations [4,5], in this study we move further to measure the evaporation heat transfer coefficients of refrigerants R-134a and R-407C in horizontal small tubes of inside diameter 2.0 and 0.83 mm. The effects of the vapor quality, refrigerant mass flux, imposed heat flux and system pressure on the evaporation heat transfer in the small tubes will be examined in detail.

2. Experimental apparatus and procedures

The experimental system modified slightly from that used in the previous study [4] is employed here to investigate the evaporation heat transfer of the HFC refrigerants in small tubes. It is schematically depicted in Fig. 1. The experimental apparatus consists of three main loops, namely, a refrigerant loop, a water-glycol loop, and a hot-water loop. The refrigerant R-134a or R-407C is circulated in the refrigerant loop. In order to control various test conditions of the refrigerants in the test section, we need to control the temperature and flow rate in the other two loops. The detailed description of the apparatus is available from our earlier study [4]. Here only the modified test section employed in the experiment is described in detail.

The modified test section along with the entry and exit sections attached to it are schematically shown in Fig. 2. Due to the tubes to be tested being relatively small, the refrigerant flow rates in them are very low and direct measurement of evaporation heat transfer coefficient in the tubes is difficult and can be subject to large error. Thus 28 small tubes all made of copper, each having the same diameter and length, are put together side by side to form a plane tube bundle acting as the test section, as shown in Fig. 2. Each small tube has the same diameter of 0.83 or 2.0 mm, outside diameter of 1.83 or 3.0 mm, and length of 150 mm. In order to allow the refrigerant to flow smoothly into the small tubes, a section including divergent, convergent and straight portions is connected to the inlets of the tubes. Besides, another section including straight and convergent parts is attached to the exits of the tubes. Both the entry and exit sections are formed by the stainless steel plates. Note that the addition of the entry and exit sections in the present study is expected to improve the flow distribution among the tubes in the bundle [5]. At the middle axial location of the small tubes 14 thermocouples are soldered onto the outer surface of the tubes. Specifically, these thermocouples are soldered onto 14 selected tubes at the circumferential position of 45° from the top of the tube or from the bottom of the tube, as shown in Fig. 3. Two copper plates of 5-mm thick are respectively soldered onto the upper and lower sides of the tube bundle also shown in Fig. 3. The copper plates are heated directly by an electric-resistance heater of 2.6-mm wide, 0.5-mm thick and 2.5-m long. The heater is connected to a 500 W DC power supply. Mica sheet is placed in the narrow space between the heater and copper plates to prevent the electric current leaking to the

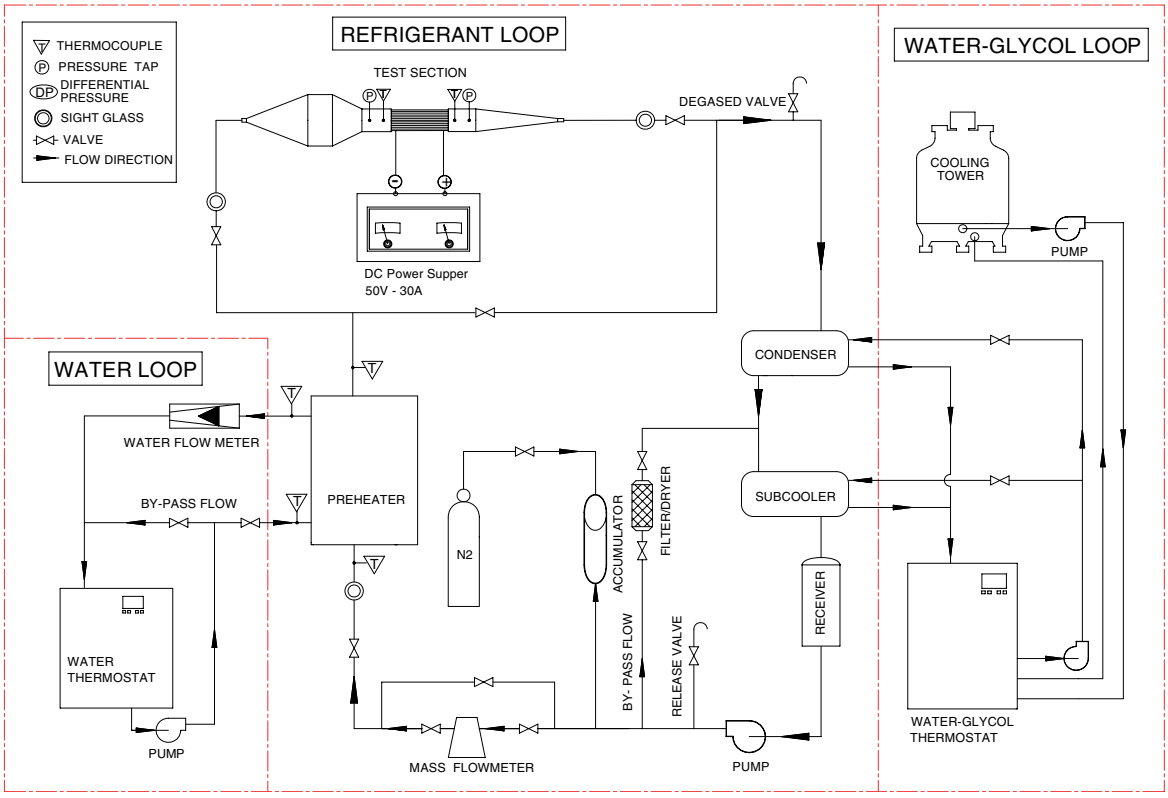

Fig. 1. Schematic layout of the experimental system.

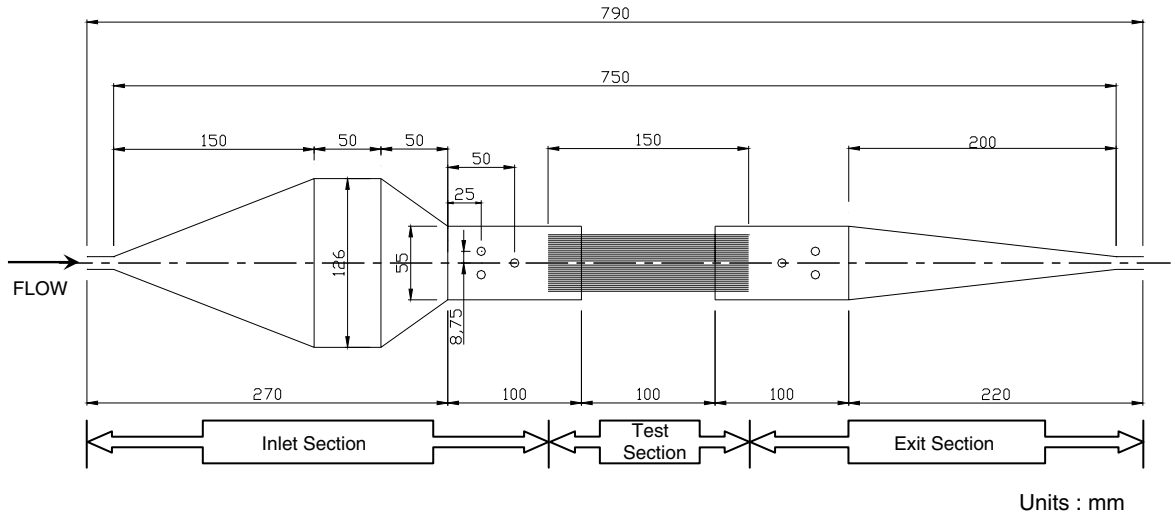

Fig. 2. Schematic diagram of test section along with the inlet and exit sections.

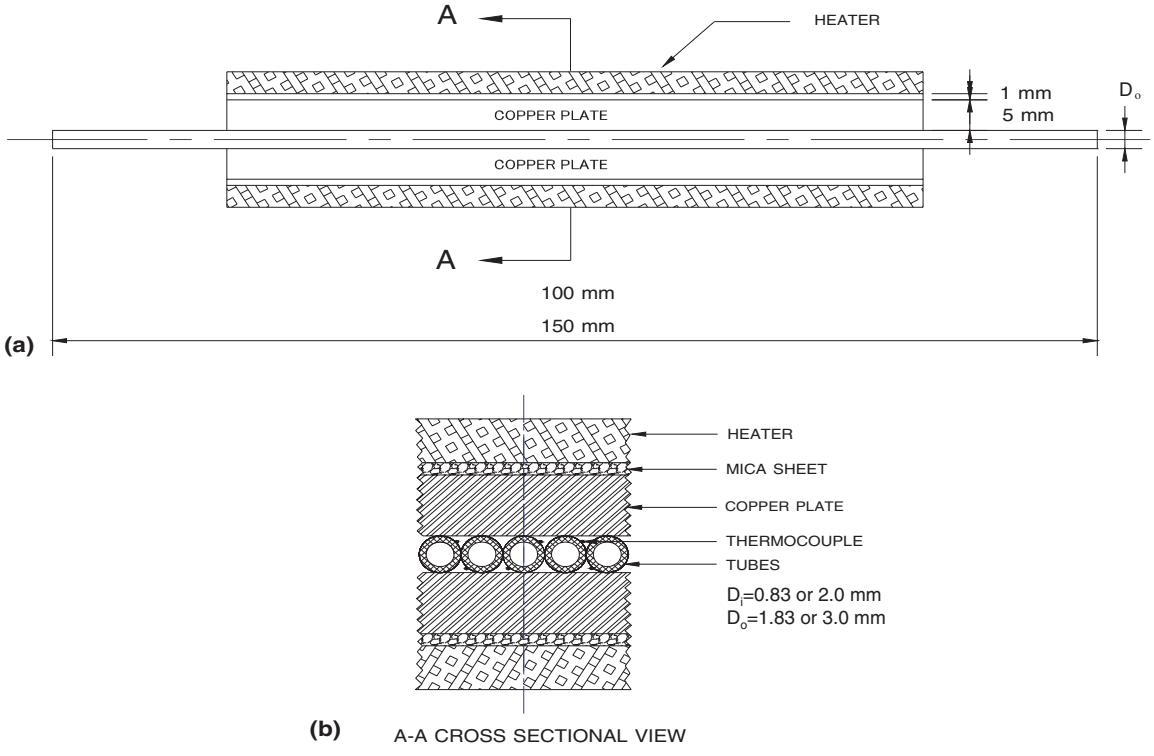

Fig. 3. Schematic diagrams showing (a) section of the small tubes and (b) locations of the thermocouples.

copper plates. The power input to the heater is measured by a power meter with an accuracy of ±0.5%. In order to reduce the heat loss from the heaters, the whole test section is wrapped with a 10-cm thick polyethylene layer. It should be noted that the heated section of the tube bundle is only 100-mm long and there are two unheated sections each having 25-mm in length upstream and downstream of the heated section. Axial heat conduction in the tube walls can be important in affecting the measured evaporation heat transfer coefficient in

view of the thermal conductivity of the copper being much higher than that of R-134a and R-407C. In the present study, however, the liquid refrigerant flow in the small tubes is at a very high Peclet number (>5000). Thus the conjugation effects between the convection in the flow and conduction in the tube walls are expected to be small, as evident from our early studies [27,28].

Before a test is started, the system temperature is compared with the saturation temperature of refrigerant R-134a or R-407C corresponding to the measured saturation pressure of the refrigerant and the allowable difference is kept in the range of 0.2–0.3 K. Otherwise, the system is re-evacuated and then re-charged to remove some noncondensible gases possibly existing in the refrigerant loop. In each test the liquid refrigerant leaving the subcooler is first maintained at a specified temperature by adjusting the water-glycol temperature and flow rate. In addition, we adjust the thermostat in the water loop to stabilize the refrigerant temperature at the test section inlet. Next, the temperature and flow rate of the water loop for the preheater are adjusted to keep the vapor quality of R-134a or R-407C at the test section inlet at the desired value. Then, we regulate the refrigerant pressure at the test section inlet by adjusting the gate valve locating right after the exit of the test section. Meanwhile, by changing the current of the DC motor connecting to the refrigerant pump, the refrigerant flow rate can be varied. The imposed heat flux from the heater to the refrigerant is adjusted by varying the electric current delivered from the DC power supply to the heater. By measuring the current delivered to and voltage drop across the heater, we can calculate the heat transfer rate to the refrigerant. All tests are run when the experimental system has reached statistically steady state. Finally, all the data channels are scanned every 5 s for a period of 50 s.

3. Data reduction

Before the two-phase experiments, the total heat loss from the test section is evaluated by comparing the total power input from the power supply with that calculated from the energy balance in the single phase refrigerant flow. The measured results indicated that for all runs in the energy balance test the heat loss was within 2%. The average single-phase liquid refrigerant convection heat transfer coefficient in the small tubes is defined as

$$h_{\mathrm{l}} = \frac{Q_{\mathrm{n}}}{A_{\mathrm{s}} \cdot (T_{\mathrm{wall}} - T_{\mathrm{r,ave}})} \tag{1}$$

Here Q_{n} is the net power input to the liquid refrigerant R134a or R-407C, A_{s} is the total inside surface area of the small tubes in the test section, T_{wall} is the average of the measured tube wall temperatures at all detected locations, and $T_{\mathrm{r,ave}}$ is the average refrigerant temperature in the tubes, which in turn is estimated from the measured refrigerant temperatures at the inlet and exit of the test section as $(T_{\mathrm{r,i}} + T_{\mathrm{r,o}})/2$.

Table 1
Summary of the uncertainty analysis

Parameter	Uncertainty
Small tubes geometry	
Length, width and thickness (%)	±1.5
Area (%)	±3.0
Parameter measurement	
Temperature, T (°C)	±0.2
Temperature difference, ΔT (°C)	±0.4
System pressure, P (kPa)	±2
Mass flux of refrigerant, G (%)	±5
Single-phase heat transfer in small tubes	
Imposed heat flux, q (%)	±4.5
Heat transfer coefficient, $h_{\mathrm{r,l}}$ (%)	±12.0
Evaporation heat transfer in small tubes	
Imposed heat flux, q (%)	±4.5
Inlet vapor quality, x_{in} (%)	±9.5
Heat transfer coefficient, h_{r} (%)	±16.0

The vapor quality of refrigerant R-134a or R-407C entering the test section is evaluated from the energy balance for the preheater. The total change of the refrigerant vapor quality in the test section is deduced from the net heat transfer rate from the heater to the refrigerant in the test section. Finally, the average heat transfer coefficient for the evaporation of refrigerant R-134a or R-407C in the test section is determined from the definition

$$h_{\mathrm{r}} \equiv \frac{Q_{\mathrm{n}}}{A_{\mathrm{s}}(T_{\mathrm{wall}} - T_{\mathrm{r,sat}})} \tag{2}$$

More detailed description of the data reduction is available from our earlier study [4]. Uncertainties of the measured heat transfer coefficients are estimated according to the procedures proposed by Kline and McClintock [29]. The detailed results from this uncertainty analysis are summarized in Table 1.

4. Results and discussion

In what follows selected data obtained here are presented to illustrate the evaporation heat transfer of R-134a or R-407C in the horizontal small circular tubes. The present experiments are performed for refrigerant R-134a or R-407C in the tube bank forming by the 2.0-mm diameter tubes with the refrigerant mass flux G varied from 200 to 400 kg/m^2 s, imposed heat flux q from 5 to 15 kW/m^2, inlet vapor quality x_{in} from 0.2 to 0.8, and refrigerant saturated temperature T_{sat} from 5 to 15 °C. While for the other tube bank forming by

the 0.83-mm diameter tubes, G is varied from 800 to 1500 kg/m^2 s with the other parameters varied in the same ranges as those for $D_i = 2.0$ mm. Note that the different ranges of the refrigerant mass flux are chosen for the different sizes of the tubes. Since at the low mass flow rate the evaporating refrigerant flow in the smaller tubes for $D_i = 0.83$ mm is somewhat unsteady, leading to the unstable intermittent flow in the system. In the following the effects of the vapor quality, imposed heat flux and refrigerant mass flux and saturated temperature on the R-134a and R-407C evaporation heat transfer coefficients are to be examined in detail.

4.1. Single phase heat transfer

Before measuring the R-134a and R-407C evaporation heat transfer coefficients, single-phase liquid R-134a and R-407C convection heat transfer coefficients in the small tubes were obtained first for the refrigerant inlet temperature fixed at 15 °C and imposed heat flux of 5 kW/m^2 with the refrigerant mass flux respectively varied from 200 to 800 kg/m^2 s (corresponding to Re_l ranging from 1786 to 9227) and from 400 to 3000 kg/m^2 s (corresponding to Re_l ranging from 1482 to 14,360) in the 2.0-mm and 0.83-mm diameter tubes. Note that the single-phase heat transfer test is conducted here to check the energy balance in the test section and the suitability of the experimental system for the present measurement. The measured single-phase liquid R-134a and R-407C heat transfer coefficients are compared with the correlations from Dittus–Boelter [30] and Gnielinski [31] in Figs. 4 and 5.

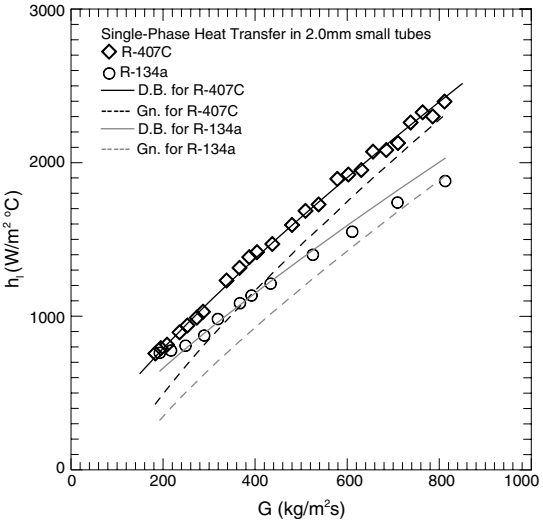

Fig. 4. Comparison of the present data for the liquid R-134a and R-407C heat transfer coefficients in 2.0-mm small tubes with the Dittus–Boelter and Gnielinski correlations.

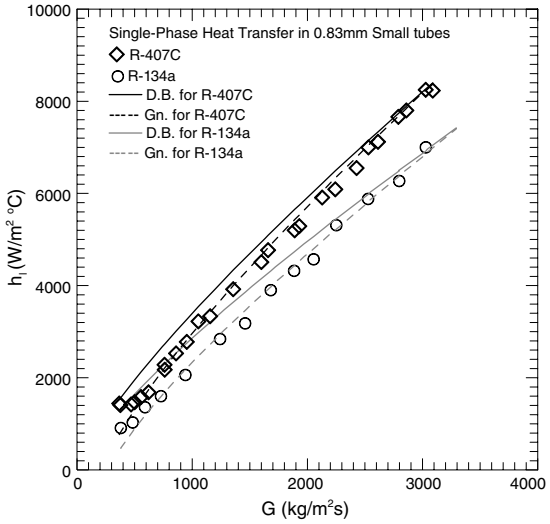

Fig. 5. Comparison of the present data for the liquid R-134a and R-407C heat transfer coefficients in 0.83-mm small tubes with the Dittus–Boelter and Gnielinski correlations.

The well known Dittus–Boelter correlation is

$$Nu_l = 0.023 \cdot Re_l^{0.8} \cdot Pr_l^{0.4} \tag{3}$$

applicable for $Re_l > 10^5$ and $0.7 < Pr_l < 16{,}700$ and the Gnielinski correlation is

$$Nu_l = \frac{(f/2)(Re_l - 1000)Pr_l}{1.07 + 12.7\sqrt{f/2}(Pr_l^{2/3} - 1)} \tag{4}$$

applicable for $2300 < Re_l < 10^6$ and $0.6 < Pr_l < 10^5$, where

$$f = (1.58 \ln Re_l - 3.28)^{-2} \tag{5}$$

It is of interest to note from the results in Figs. 4 and 5 that for the 2.0-mm tubes the measured single-phase heat transfer coefficients are close to the Dittus–Boelter correlation. While for the 0.83-mm tubes the data are well fitted with the Gnielinski correlation. Finally, in the single-phase heat transfer tests to check the energy balance in the test section the relative heat loss is found to be within 2% for all runs. Thus the heat loss from the test section is small.

4.2. Evaporation heat transfer in 2.0-mm tubes

The measured heat transfer data for the R-134a and R-407C evaporation in the 2.0-mm tubes are presented first. Figs. 6 and 7 respectively illustrate how the refrigerant saturated temperature, mass flux and imposed heat flux affect the heat transfer coefficients for R-134a and R-407C evaporation in the 2.0-mm tubes. The measured heat transfer coefficients are examined by checking their variations with the vapor quality at the test section inlet x_{in}. Since the tubes are short, the total quality change Δx between the inlet and exit of the test section is relatively

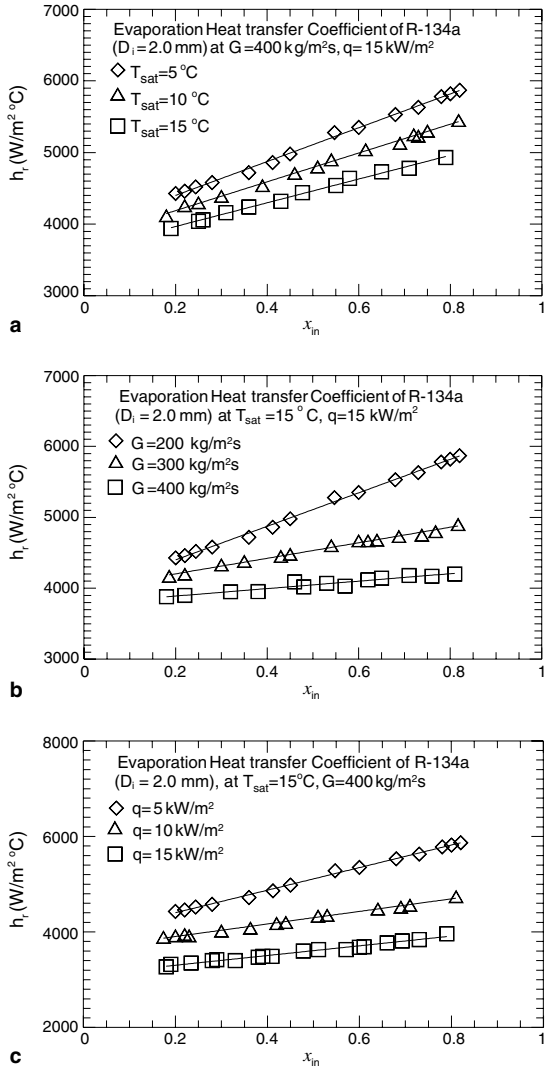

Fig. 6. Variations of R-134a evaporation heat transfer coefficient with inlet vapor quality in 2.0-mm small tubes: (a) for various T_{sat} at $G = 400$ kg/m^2 s and $q = 15$ kW/m^2, (b) for various G at $T_{sat} = 15$ °C and $q = 15$ kW/m^2, and (c) for various q at $T_{sat} = 15$ °C and $G = 400$ kg/m^2 s.

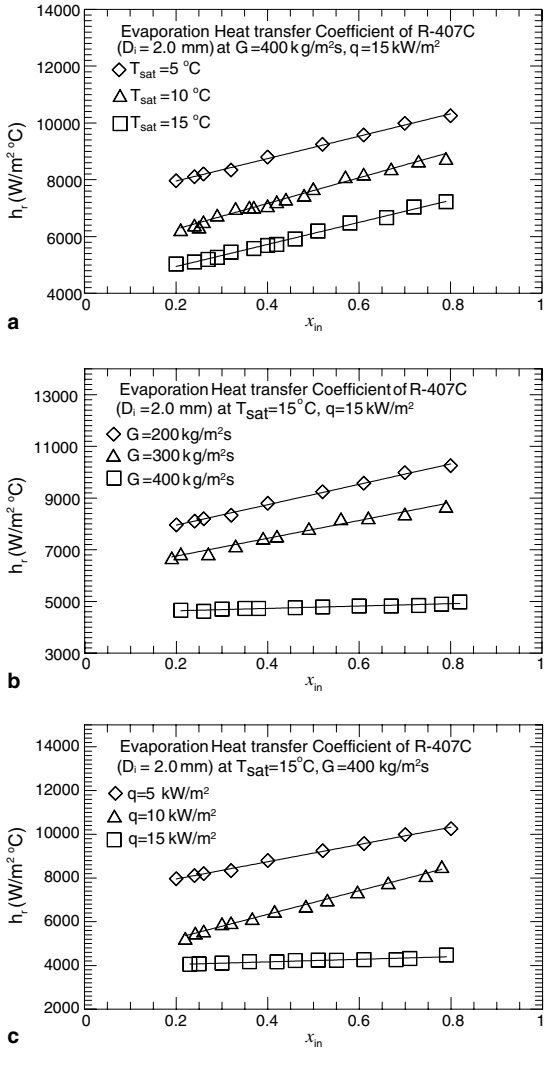

Fig. 7. Variations of R-407C evaporation heat transfer coefficient with inlet vapor quality in 2.0-mm small tubes: (a) for various T_{sat} at $G = 400$ kg/m^2 s and $q = 15$ kW/m^2, (b) for various G at $T_{sat} = 15$ °C and $q = 15$ kW/m^2, and (c) for various q at T_{sat}=15 °C and $G = 400$ kg/m^2 s.

small, ranging from 0.01 to 0.03 in the present study. The results given in Figs. 6 and 7 show that for given q, T_{sat} and G the evaporation heat transfer coefficients for both R-134a and R-407C increase almost linearly with the inlet quality. Moreover, at higher T_{sat}, q and G the increase of h_r with x_{in} is more significant. The significant increase of the evaporation heat transfer coefficients with the inlet vapor quality is considered to result from the fact that at a higher inlet quality the liquid film thickness of the refrigerant on the inside surface of the tubes becomes thinner. Hence the thermal resistance of the liquid film is reduced and heat transfer across the film is improved. Besides, at a higher vapor quality the mass flux of the vapor and the velocity of vapor flow are faster. This also improves the interfacial heat transfer. More specifically for the case with R-134a at $T_{sat} = 15$ °C, $G = 400$ kg/m^2 s and $q = 15$ kW/m^2, an increase of 31% in h_r occurs for x_{in} raised from 0.2 to 0.8 (Fig. 6(a)). The effects of each parameter on h_r are examined in the following. At first, the effects of the saturated temperature T_{sat} are presented in Fig. 6(a) by showing the variations of the R-134a evaporation heat transfer coefficients with the inlet vapor quality at $T_{sat} = 5$, 10, 15 °C for given refrigerant mass flux and imposed heat flux. The results in Fig. 6(a) indicate that at fixed q

and G the R-134a evaporation heat transfer coefficients rise with the saturated temperature of the refrigerant. A similar trend is also noted by Agostini and Bontemps [6]. This increase in h_r with T_{sat} is ascribed to the fact that at a higher T_{sat} the latent heat of vaporization i_{fg} is lower, which in turn results in a higher evaporation rate of the liquid R-134a for a fixed q. Hence the R-134a vapor in the tubes flows at a higher speed, producing a higher convection effect and therefore a higher h_r. To be more quantitative on the effects of T_{sat} on the R-134a evaporation heat transfer coefficient, the quality-averaged evaporation heat transfer coefficients $\bar{h}_r$ at $G = 400$ kg/m^2 s and $q = 15$ kW/m^2 are calculated from the data in Fig. 6(a). For T_{sat} raised from 5 °C to 15 °C, $\bar{h}_r$ is increased by 19%.

Next, the effects of the refrigerant mass flux on the R-134a evaporation in the 2.0-mm tubes are shown in Fig. 6(b). The results indicate that the increase of h_r with the R-134a mass flux is rather significant, suggesting that the interfacial evaporation is effectively enhanced by the rise in the refrigerant mass flux. Hence the convection mechanism is important in the flow. Quantitatively according to the data in Fig. 6(b) for $T_{sat} = 15$ °C and $q = 15$ kW/m^2, the quality-averaged evaporation heat transfer coefficient is increased by 27% for G raised from 200 to 400 kg/m^2 s for R-134a.

Then, the results presented in Fig. 6(c) indicate that the R-134a evaporation heat transfer coefficient increases rather significantly with the imposed heat flux. This significant increase of h_r with q reflects that the evaporation at the liquid–vapor interface in the refrigerant flow is substantially augmented by the increase in the imposed heat flux. According to the data in Fig. 6(c) for $T_{sat} = 15$ °C and $G = 400$ kg/m^2 s, with q raised from 5 to 15 kW/m^2 $\bar{h}_r$ is increased by 44%.

Checking with the heat transfer data given in Fig. 7 for R-407C, we note that the effects of the vapor quality, refrigerant saturated temperature and mass flux, and imposed heat flux on the evaporation heat transfer coefficients of R-407C are qualitatively similar to those for R-134a. A close inspection of the data in Figs. 6 and 7, however, reveals some differences. The R-407C evaporation heat transfer coefficient is noticeably higher. Besides, the effects of T_{sat}, G and q on h_r for R-407C are stronger for most cases. Moreover, for R-134a the evaporation heat transfer coefficient varies with G more significantly at a high refrigerant mass flux (Fig. 6(b)). While the opposite is the case for R-407C, as evident from Fig. 7(b).

4.3. Evaporation heat transfer in the smaller tubes ($D_i = 0.83$ mm)

The measured heat transfer data for the smaller tubes with $D_i = 0.83$ mm are illustrated in Fig. 8 for the R-134a evaporation and in Fig. 9 for the R-407C evaporation, covering the effects of various parameters on the evaporation heat transfer coefficients for these two refrigerants. First, it is noted from the results in Fig. 8 that for given T_{sat}, G and q the R-134a evaporation heat transfer coefficient also increases noticeably with the inlet vapor quality except at high vapor quality for some cases at low G and high q (Fig. 8(b)). A close inspection of data in Fig. 8 reveals that at low mass flux and high imposed heat flux, h_r even decreases with a rise in x_{in} at a high vapor quality for $x_{in} > 0.6$. This is conjectured to result from the partial dryout of the refrigerant on the tube wall at high x_{in} at these conditions. In fact, the data

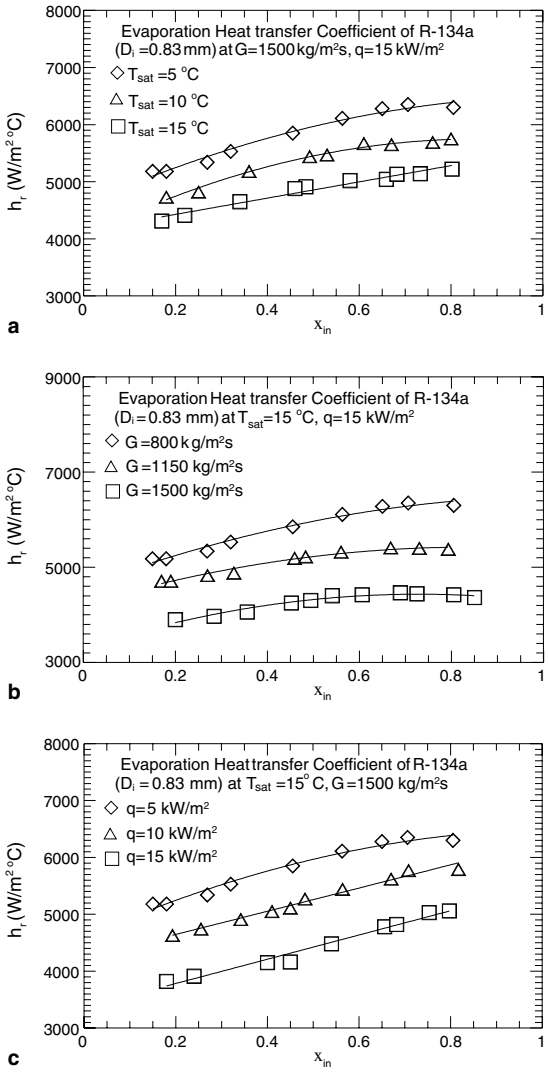

Fig. 8. Variations of R-134a evaporation heat transfer coefficient with inlet vapor quality in 0.83-mm small tubes: (a) for various T_{sat} at $G = 1500$ kg/m^2 s and $q = 15$ kW/m^2, (b) for various G at $T_{sat} = 15$ °C and $q = 15$ kW/m^2, and (c) for various q at $T_{sat} = 15$ °C and $G = 1500$ kg/m^2 s.

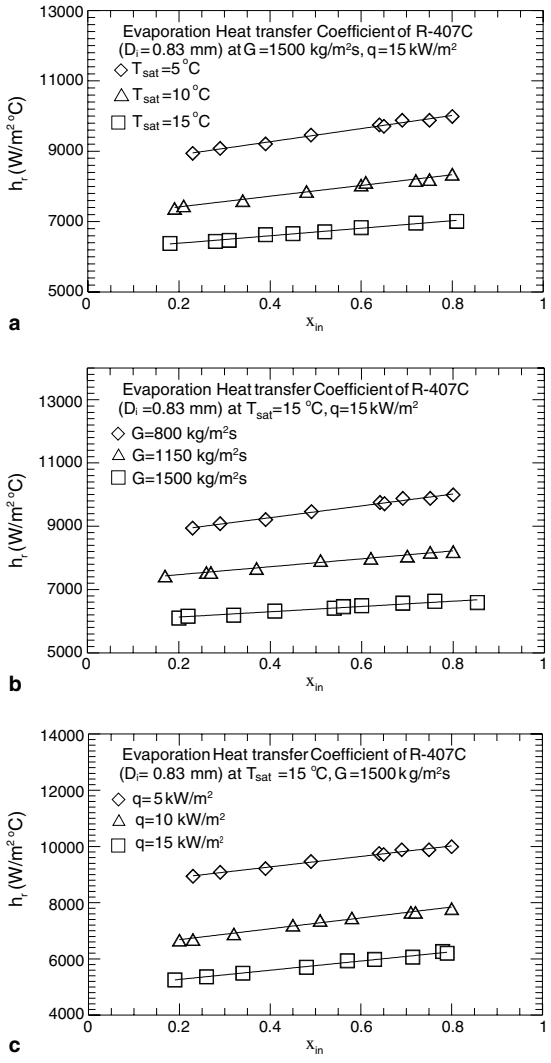

Fig. 9. Variations of R-407C evaporation heat transfer coefficient with inlet vapor quality in 0.83-mm small tubes: (a) for various T_{sat} at $G = 1500\ kg/m^2\ s$ and $q = 15\ kW/m^2$, (b) for various G at $T_{sat} = 15\ °C$ and $q = 15\ kW/m^2$, and (c) for various q at $T_{sat} = 15\ °C$ and $G = 1500\ kg/m^2\ s$.

from Yan and Lin [4] for R-134a evaporation in the 2.0-mm tubes show the decline of h_r with a rise in x_{in} for many cases. These earlier poor data result from the significant refrigerant dryout in the tubes, as already mentioned here. This is apparently due to the bad refrigerant mass flux distribution at the inlet of the previous test section. In the present study, this bad flow distribution has been improved by modifying the entry and exit sections of the test section. Hence the partial refrigerant dryout only occurs in the smaller tubes with $D_i = 0.83$ mm at high x_{in} and q and low G (Fig. 8(b)). Moreover, at an intermediate quality the increase of h_r with x_{in} is rather large for the cases at high T_{sat}, q and G. However, for these cases the increase is rather mild at low quality. Quantitatively for the case with $T_{sat} = 15\ °C$, $G = 1500\ kg/m^2\ s$ and $q = 15\ kW/m^2$, the increase in h_r is 24% for x_{in} raised from 0.2 to 0.8 (Fig. 8(a)).

According to the results in Fig. 9, the R-407C evaporation heat transfer coefficients increase almost linearly with the inlet vapor quality for most cases. The increase is also rather substantial at high T_{sat}, q and G. Checking the numerical values for h_r in Fig. 9 reveals the quantitative increase of h_r with x_{in} for R-407C. For example, at $T_{sat} = 15\ °C$, $G = 1500\ kg/m^2\ s$ and $q = 15\ kW/m^2$ we have a much smaller h_r increase of 11% for R-407C for the same rise in x_{in} (Fig. 9(a)).

An overall inspection of the data presented in Fig. 8 discloses that for R-134a evaporation in the smaller tubes with $D_i = 0.83$ mm the evaporation heat transfer in the flow can be significantly increased by raising the refrigerant saturated temperature, mass flux and heat flux. These trends are similar to that for the large tubes with $D_i = 2.0$ mm already examined above. A further inspection of the measured data for R-134a evaporation in the smaller tubes reveals that the effects of the refrigerant saturated temperature and mass flux on h_r are more pronounced at a higher heat flux. Finally, the heat flux variation on h_r is more important at high T_{sat} and G.

For R-407C evaporation in the smaller tubes a substantial increase in h_r with the increasing refrigerant saturated temperature, mass flux and heat flux is also noted from the results in Fig. 9. It should be mentioned that for R-407C evaporation at high vapor quality h_r does not decline for a rise in x_{in}, unlike that for R-134a. This is attributed to the fact that R-407C has a high latent heat of vaporization and the partial dryout on the tube wall is less likely to occur in the R-407C evaporation. Moreover, in the smaller tubes the effects of T_{sat}, G and q on the evaporation heat transfer coefficients for R-407C are also stronger than that for R-134a. Again in the small tubes R-407C has a higher h_r.

To be more quantitative on the effects of various parameters on the heat transfer data in the smaller tubes, the quality-averaged evaporation heat transfer coefficients for various cases are evaluated. The results from this evaluation show that for R-134a at $G = 1500\ kg/m^2\ s$ and $q = 15\ kW/m^2$, $\bar{h}_r$ experiences a 21% increase when T_{sat} is raised from 5 °C to 15 °C (Fig. 8(a)). While for R-407C the corresponding increase is 37% (Fig. 9(a)). Next, we note that for R-134a at $T_{sat} = 15\ °C$ and $q = 15\ kW/m^2$, there is a 41% increase in $\bar{h}_r$ for G raised from 800 to 1500 $kg/m^2\ s$ (Fig. 8(b)). The corresponding increase for R-407C is 48% (Fig. 9(b)). Finally, a 33% increase in $\bar{h}_r$ is noted for q raised from 5 to 15 kW/m^2 for R-134a at $T_{sat} = 15\ °C$ and $G = 1500\ kg/m^2\ s$ (Fig. 8(c)). For R-407C the corresponding increase is 67% (Fig. 9(c)).

4.4. Correlation equation for evaporation heat transfer coefficients

For practical application the present data for the R-134a and R-407C evaporation in the 2.0-mm and 0.83-mm tubes need to be correlated empirically. The data presented above indicate that $\bar{h}_r$ varies linearly with the vapor quality for most cases and the correlation is thus expressed as

$$Nu_r \equiv \frac{h_r \cdot D_i}{k_l} = m_1 x_{in} + m_2 \tag{6}$$

where m_1 and m_2 can be correlated as

$$m_1 = f(Bo, Re) = a_1 + b_1 Bo^{c_1} Re^{d_1} \tag{7}$$

$$m_2 = f(Bo, Re) = a_2 Bo^{b_2} Re^{c_2} \tag{8}$$

The values for the coefficients in m_1 and m_2 are $a_1 = 1.39$, $b_1 = 1.87 \times 10^{-3}$, $c_1 = 1.82$, $d_1 = 3.14$, $a_2 = 28.6$, $b_2 = 0.706$, $c_2 = 0.888$. The Boiling number and Reynolds number are defined respectively as

$$Bo = \frac{q}{G \cdot i_{fg}} \tag{9}$$

$$Re_{=} \frac{G \cdot D_i}{\mu_l} \tag{10}$$

Comparison of the above correlation with the present experimental data shown in Fig. 10 indicates that more than 80% of the present data for h_r fall within ±35% of Eq. (6), and the mean absolute error (MAE) between the present data for h_r and the proposed correlation is 19%.

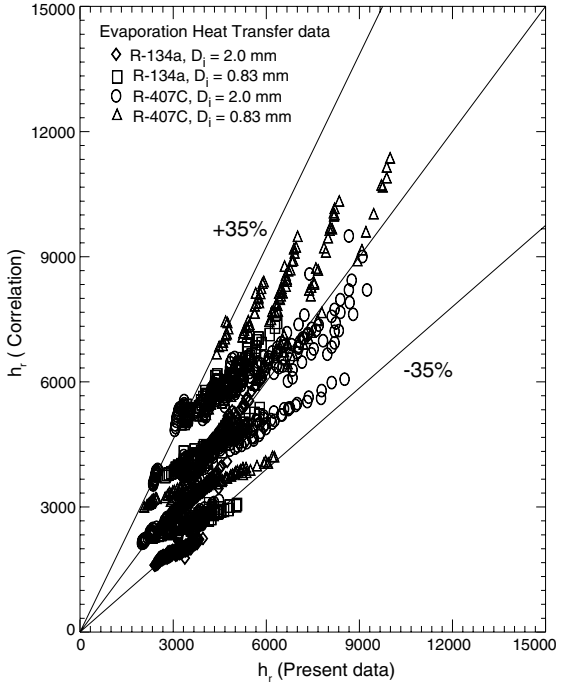

Fig. 10. Comparison of the measured data for heat transfer coefficient for the evaporation of R-134a and R-407 in 0.83-mm and 2.0-mm small tubes with the proposed correlation.

5. Concluding remarks

Experiments have been conducted here to investigate the evaporation heat transfer of R-134a and R-407C in the small tubes with $D_i = 0.83$ and 2.0 mm. The effects of the refrigerant saturated temperature, mass flux, imposed heat flux, and vapor quality of R-134a and R-407C on the evaporation heat transfer coefficients have been examined in detail. The results show that the R-134a and R-407C evaporation heat transfer coefficients in the small tubes increase almost linearly with the vapor quality and the increases are significant except at low imposed heat flux and low refrigerant mass flux. Moreover, the increases of the R-134a and R-407C evaporation heat transfer coefficients in both tubes with the imposed heat flux, refrigerant mass flux and saturated temperature are also substantial. Besides, the evaporation heat transfer coefficients for R-134a are noticeably lower than that for R-407C at the same T_{sat}, G and q. Furthermore, for R-134a in the smaller tubes ($D_i = 0.83$ mm) partial refrigerant dryout may occur, resulting in the decline of the evaporation heat transfer coefficient at increasing inlet vapor quality at high x_{in}. This is normally seen at high imposed heat flux and saturated temperature and low mass flux. Finally, an empirical correlation is proposed to correlate the present data for R-134a and R-407C evaporation heat transfer coefficients in the small tubes.

Acknowledgements

The financial support of this study by the engineering division of National Science Council of Taiwan, ROC through the contract NSC 92-2212-E-009-016 is greatly appreciated.

References

[1] M.H. Kim, S.Y. Lee, S.S. Mehendale, R.L. Webb, Microchannel heat exchanger design for evaporator and condenser applications, Adv. Heat Transfer 37 (2003) 297–429.

[2] W. Yu, D.M. France, M.W. Wambsganss, J.R. Hull, Two-phase pressure drop, boiling heat transfer, and critical heat flux to water in a small-diameter horizontal tube, Int. J. Multiphase Flow 28 (6) (2002) 927–941.

[3] B. Sumith, F. Kaminaga, K. Matsumura, Saturated flow boiling of water in a vertical small diameter tube, Exper. Thermal Fluid Sci. 27 (7) (2003) 789–801.

[4] Y.Y. Yan, T.F. Lin, Evaporation heat transfer and pressure drop of refrigerant R-134a in a small pipe, Int. J. Heat Mass Transfer 41 (24) (1998) 4183–4194.
[5] Y.Y. Yan, T.F. Lin, Reply to Prof. R.L. Webb's and Dr. J.W. Paek's comments, Int. J. Heat Mass Transfer 46 (6) (2003) 1111–1113.
[6] B. Agostini, A. Bontemps, Vertical boiling of refrigerant R-134a in small channels, Int. J. Heat Fluid Flow 26 (2005) 296–306.
[7] V.G. Nino, P.S. Hrnjak, T.A. Newell, Two-phase flow visualization of R-134a in a multiport microchannel tube, Heat Transfer Eng. 24 (1) (2003) 41–52.
[8] Y. Fujita, Y. Yang, N. Fujita, Flow boiling heat transfer and pressure drop in uniformly heated small tubes, in: Proceedings of the Twelfth International Heat Transfer Conference, vol. 3, 2002, pp. 743–748.
[9] G.M. Lazarek, S.H. Black, Evaporative heat transfer, pressure drop and critical heat flux in a small vertical tube with R-113, Int. J. Heat Mass Transfer 25 (7) (1982) 945–960.
[10] S. Lin, P.A. Kew, K. Cornwell, Two-phase heat transfer to a refrigerant in a 1 mm diameter tube, Int. J. Refrig. 24 (1) (2001) 51–56.
[11] S. Lin, P.A. Kew, K. Cornwell, Flow boiling of refrigerant R141b in small tubes, Chem. Eng. Res. Des. 79 (A4) (2001) 417–424.
[12] K. Cornwell, P.A. Kew, Boiling in small parallel channels, in: Proceedings of the International Conference on Energy Efficiency in Process Technology, Elsevier Applied Science, Athens, Greece, 1992, pp. 624–638.
[13] P.A. Kew, K. Cornwell, Correlations for the prediction of boiling heat transfer in small-diameter channels, Appl. Thermal Eng. 17 (8–10) (1997) 705–715.
[14] T.N. Tran, M.W. Wambsganss, D.M. France, Small circular- and rectangular-channel boiling with two refrigerants, Int. J. Multiphase Flow 22 (3) (1996) 485–498.
[15] Z.Y. Bao, D.F. Fletcher, B.S. Haynes, Flow boiling heat transfer of Freon R11 and HCFC123 in narrow passages, Int. J. Heat Mass Transfer 43 (18) (2000) 3347–3358.
[16] M.W. Wambsganss, D.M. France, J.A. Jendrzejczyk, T.N. Tran, Boiling heat transfer in a horizontal small-diameter tube, ASME J. Heat Transfer 115 (4) (1993) 963–972.
[17] G.R. Warrier, V.K. Dhir, L.A. Momoda, Heat transfer and pressure drop in narrow rectangular channels, Exper. Thermal Fluid Sci. 26 (1) (2002) 53–64.
[18] H. Oh, M. Katsuta, K. Shibata, Heat transfer characteristics of R134a in a capillary tube heat exchanger, in: Proceedings of 11th International Heat Transfer Conference, vol. 6, 1998, pp. 131–136.
[19] J. Pettersen, Flow vaporization of CO_2 in microchannel tubes, Exper. Thermal Fluid Sci. 28 (2–3) (2004) 111–121.
[20] S.M. Ghiaasiaan, S.I. Abdel-khalik, Two-phase flow in microchannels, Adv. Heat Transfer 34 (2001) 145–254.
[21] J.R. Thome, Boiling in microchannels: a review of experiment and theory, Int. J. Heat Fluid Flow 25 (2) (2004) 128–139.
[22] C.B. Sobhan, S.V. Garimella, A comparative analysis of studies on heat transfer and fluid flow in microchannels, Microscale Thermophys. Eng. 5 (4) (2001) 293–311.
[23] S.G. Kandkikar, Two-phase flow patterns, pressure drop, and heat transfer during boiling in minichannel flow passages of compact evaporators, Heat Transfer Eng. 23 (1) (2002) 5–23.
[24] S.G. Kandlikar, Heat transfer mechanisms during flow boiling in microchannels, ASME J. Heat Transfer 126 (1) (2004) 8–16.
[25] B. Watel, Review of saturated flow boiling in small passages of compact heat-exchangers, Int. J. Thermal Sciences 42 (2) (2003) 107–140.
[26] C. Vlasie, H. Macchi, J. Guilpart, B. Agostini, Flow boiling in small diameter channels, Int. J. Refrig. 27 (2004) 191–201.
[27] T.F. Lin, J.C. Kuo, Transient conjugated heat transfer in fully-developed laminar pipe flows, Int. J. Heat Mass Transfer 31 (5) (1988) 1093–1102.
[28] J.C. Kuo, T.F. Lin, Steady conjugated heat transfer in fully-developed laminar pipe flows, ASME/AIAA J. Thermophys. Heat Transfer 2 (1988) 281–283.
[29] S.J. Kline, F.A. McClintock, Describing uncertainties in single-sample experiments, Mech. Eng. 75 (1953) 3–8.
[30] F.W. Dittus, L.M.K. Boelter, Heat transfer in automobile radiator of the tube type, Publication in Engineering, University of California, Berkley, vol. 2, 1930, p. 250.
[31] V. Gnielinski, New equations for heat and mass transfer in turbulent pipe and channel flow, Int. Chem. Eng. 16 (2) (1976) 359–368.